Related Commentary on page 363

American Journal of Pathology, Vol. 168, No. 2, February 2006

DOI: 10.2353/ajpath.2006.050677

Tumorigenesis and Neoplastic Progression

Remodeling of the Mammary Microenvironment after Lactation Promotes Breast Tumor Cell Metastasis

Shauntae M. McDaniel,* Kristen K. Rumer,† Sandra L. Biroc,‡ Richard P. Metz,§ Meenakshi Singh,¶ Weston Porter,§ and Pepper Schedin*†‖**

From the AMC Cancer Research Center, Denver, Colorado; the Department of Medicine,† Division of Medical Oncology, the Program of Cell and Developmental Biology,‖ the Department of Pathology,¶ the University of Colorado Cancer Center,** University of Colorado Health Science Center, Aurora, Colorado; Berlex Biosciences Pharmaceuticals,‡ Richmond, California; and the Department of Interactive Biosciences,§ Texas A&M, College Station, Texas*

The mammary gland microenvironment during postlactational involution shares similarities with inflammation, including high matrix metalloproteinase activity, fibrillar collagen deposition, and release of bioactive fragments of fibronectin and laminin. Because inflammation can promote tumorigenesis, we evaluated whether the tissue microenvironment of the involuting gland is also promotional. Extracellular matrix was isolated from mammary glands of nulliparous rats or rats with mammary glands undergoing weaning-induced involution. Using these matrices as substratum, nulliparous matrix was found to promote ductal organization of normal mammary epithelial MCF-12A cells in three-dimensional culture and to suppress invasion of mammary tumor MDA-MB-231 cells in transwell filter assays. Conversely, involution matrix failed to support ductal development in normal cells and promoted invasiveness in tumor cells. To evaluate the effects of these matrices on metastasis *in vivo*, MDA-MB-231 cells, premixed with Matrigel, nulliparous matrix, or involution matrix, were injected into mammary fat pads of nude mice. Metastases to lung, liver, and kidney were increased in the involution matrix group, and correlated with a twofold increase in tumor vascular endothelial growth factor expression and increased angiogenesis. These data suggest that the mammary gland microenvironment becomes promotional for tumor cell dissemination during involution, thus providing a plausible mechanism to explain the high rate of metastases that occur with pregnancy-associated breast cancer. ***(Am J Pathol 2006, 168:608–620; DOI: 10.2353/ajpath.2006.050677)***

Evidence that pathological changes in the tumor microenvironment promote tumorigenesis has been obtained in experimental model systems and clinical settings.[1–6] Specifically, the tissue microenvironments associated with wound healing and inflammation correlate with tumor promotion and progression. Prominent changes in the microenvironment that occur with wound healing and inflammation include activation of fibroblasts, endothelial cells, and immune cells. These activated mesenchymal cells secrete cytokines, growth factors, tissue-remodeling enzymes, and provisional extracellular matrix (ECM) molecules, all of which facilitate wound closure and remodeling of the damaged tissue. Like mesenchymal cells, tumor cells can also be stimulated by the proinflammatory microenvironment. For example, individuals with *Helicobacter pylori* infection or Crohn's disease have chronic inflammation of the gastric and intestinal mucosa, which correlates with a significantly increased risk for stomach and colon cancers, respectively.[6] Similarly, smoking-induced inflammation of the lung and inflammation of unknown etiology in the prostate also correlate with disease progression at these sites.[7,8] In experimental settings, newly hatched chicks injected with Rous sarcoma virus only develop secondary tumors at sites of wounding.[9] In a murine model, mammary tumors arise when nontumorigenic mammary epithelial cells are engrafted into a stroma wounded by irradiation but not when engrafted into nonirradiated stroma.[10] Further evidence that pathological changes in tissue stroma can promote epithelial cell transformation has been obtained from experiments studying the effects of genetically modified stromal cells on epithelial cell function. Mammary fibroblasts modified to overexpress transforming growth

Supported by a grant from the National Cancer Institute (R01 CA85944 to P.S.).

S.M.M. and K.K.R. contributed equally to this work.

Accepted for publication October 24, 2005.

Address reprint requests to Pepper Schedin, Ph.D., Division of Medical Oncology, Mail Stop 8117, P.O. Box 6511, UCHSC, Aurora, CO 80045. E-mail: pepper.schedin@uchsc.edu.

factor-β or hepatocyte growth factor promote tumor formation of histologically normal human mammary epithelial cells, whereas unmodified fibroblasts did not.[11] Further, neoplastic transformation of rat mammary epithelial cells transplanted into mammary stroma occurred only when the stroma had been exposed *in vivo* to chemical carcinogen.[12] These studies clearly establish that pathological changes in the tumor cell microenvironment contribute to cancer development.

The role of physiological changes in the tissue microenvironment on cancer development has not been investigated to the same extent as pathological changes. One reason for the lack of data in this area is that the stroma in mature, adult tissues has been thought to primarily provide a structural support function. Thus, stroma was not expected to undergo physiologically induced changes sufficient to influence tumorigenesis. The mammary gland is a unique organ in which to investigate the questions of whether stromal composition and function are physiologically altered and whether these changes impact tumorigenesis. This is because the form and function of normal mammary epithelium changes dramatically with reproductive state, and concomitant changes in the stroma might be anticipated.[13] In our laboratory we have focused on characterizing physiological alterations in the mammary microenvironment that accompany pregnancy, lactation, and weaning-induced involution of the mammary gland. We and others have found that the composition and function of the mammary ECM are coordinated with, and appear to facilitate mammary epithelial cell proliferation, differentiation, and death that occur during the pregnancy, lactation, and involution cycle.[13,14] Thus, the tissue microenvironment in the normal mammary gland varies dramatically with reproductive state.[13] Consequently, the physiologically normal mammary microenvironment may also vary in its ability to support the development of breast cancer.

Characterization of the microenvironment that accompanies regression of mammary epithelium after lactation has identified similarities with provisional wound-healing stroma.[13,15–17] The lactating breast is composed primarily of epithelium committed to the secretion of milk proteins. With weaning, the mammary gland undergoes involution, a process involving dramatic tissue remodeling and massive death of the secretory epithelium. The stroma from mammary glands undergoing weaning-induced involution has elevated matrix metalloproteinase (MMP) activity,[17,18] high levels of fibrillar collagen,[13] and bio-active proteolytic fragments of laminin[13,19,20] and fibronectin,[13,15,17] all of which are attributes of wound-healing stroma. Thus, physiological tissue remodeling of the mammary gland appears to use some of the same remodeling programs that are activated during wound healing, and like wound-healing stroma, may have tumor-promoting activity. To investigate this hypothesis, mammary gland ECM was isolated from quiescent mammary glands of nulliparous and weaning-induced involuting rat mammary glands. The effects of these isolated matrices on the metastatic potential of breast cancer cells were evaluated using *in vitro* and *in vivo* models. Our data suggest that the microenvironment of the mammary gland during weaning-induced involution is tumor promotional and may represent a window of opportunity for tumor cell metastasis.

Materials and Methods

Rat Breeding, Reproductive Staging, and Histology

Female Sprague-Dawley rats, 77 days of age (Harlan-Tekland, Indianapolis, IN), were bred as previously described.[13] Two days after parturition, litter sizes were normalized to eight pups, and pups were removed after 10 days of lactation to initiate gland involution. Mammary glands were harvested on days 4, 5, or 6 after weaning from nine animals. For the quiescent control group, inguinal mammary gland chains 4 to 6 were harvested from 12 age-matched nulliparous rats. Lymph node-free inguinal mammary glands were snap-frozen and stored at −80°C for subsequent matrix isolation and biochemical analyses. To control for variations in ECM composition that may accompany estrous cycling in the nulliparous rats, phase of estrous cycle was determined by daily cervical lavages, and all nulliparous rats were sacrificed in the estrus phase of the cycle, as previously described.[21] Mammary tissue associated with the dissected lymph region was fixed in 10% neutral-buffered formalin for 18 hours, paraffin-embedded, cut into 5-μm sections, and stained with hematoxylin and eosin (H&E). The changes in mammary tissue in relation to the reproductive stage were evaluated histologically. For detection of fibrillar collagen, 5-μm sections of mammary tissue were stained with Sirius Red F3B according to published methods[22] and counterstained with Weigert's iron hematoxylin. All animal procedures were performed in compliance with the AMC Cancer Research Institute Animal Care and Use Committee and National Institutes of Health Policy on Humane Care and Use of Laboratory Animals.

Mammary ECM Isolation

Mammary matrix isolation was performed based on a previously described protocol,[13] using pooled inguinal mammary gland tissue from at least six rats per group. Briefly, frozen inguinal mammary glands, with lymph nodes removed, were pulverized and extracted in a high-salt/*N*-ethylmaleimide solution (3.4 mol/L NaCl, 50 mmol/L Tris-HCl, pH 7.4, 4 mmol/L ethylenediaminetetraacetic acid, 2 mmol/L *N*-ethylmaleimide) containing proteinase inhibitor cocktail (100 μg/ml phenylmethyl sulfonyl fluoride, 50 μg/ml each aprotinin, leupeptin, and pepstatin), at 4°C. Homogenates were enriched for ECM by two cycles of centrifugation (RCF_{max} 110,000 $\times$ *g*, 30 minutes, 4°C), and pellets resuspended in high-salt/*N*-ethylmaleimide buffer. ECM-enriched pellets were resuspended in mid-salt/urea solution (2 mol/L urea, 0.2 mol/L NaCl, 50 mmol/L Tris-HCl, pH 7.4, 4 mmol/L ethylenediaminetetraacetic acid, 2 mmol/L *N*-ethylmaleimide) with proteinase inhibitor cocktail and extracted overnight at 4°C. Samples were pelleted at RCF_{max} 110,000 $\times$ *g*, and the ECM-enriched supernatants extensively dialyzed (MWCO 12–14,000 kd; Spectrum Lab, Rancho

Dominguez, CA) against low-salt buffer (0.15 mol/L NaCl, 50 mmol/L Tris-HCl, pH 7.4, 4 mmol/L ethylenediaminetetraacetic acid), followed by dialysis against serum-free media [Dulbecco's modified Eagle's medium/F12 media (Sigma Chemical Co., St. Louis, MO) supplemented with 1 μg/ml gentamicin] at 4°C. Matrices were stored on ice at 4°C and used within 2 weeks of isolation. As reported previously, ECM protein integrity is stable under these storage conditions.[13] For the *in vitro* studies, all experiments were performed in duplicate with two distinct batches of matrices.

Western Blot Analysis

Tissue and ECM from nulliparous and involution glands were analyzed by Western blot as previously described.[13] The following antibodies were used: polyclonal rabbit anti-rat fibronectin (1:250; Life Technologies, Inc., Gaithersburg, MD), polyclonal rabbit anti-laminin (1:500; Novus Biologicals, Littleton, CO), and protein A secondary antibody (1:10,000; Amersham, Piscataway, NJ). Monoclonal mouse anti-actin (1:500; Amersham) followed by an anti-mouse secondary antibody (1:5000; Santa Cruz Biotechnology, Santa Cruz, CA) was used for protein loading controls. Signal was obtained using an enhanced chemiluminescence Western detection kit (Amersham). For fibronectin Western blots, 3.3 μg of respective matrix were loaded per lane. For laminin Western blots and zymogen assays, 9.5 μg of respective matrices were loaded per lane. Coomassie Blue R250 staining of total protein was used to validate equal protein loading.

Cell Lines

MCF-12A cells were obtained from American Type Culture Collection (Manassas, VA). These are a nontumorigenic human immortalized mammary epithelial cell line.[23] For routine maintenance, MCF-12A cells were grown in complete media consisting of Ham's F12/Dulbecco's modified Eagle's medium (Life Technologies, Inc., Carlsbad, CA) containing 100 ng/ml cholera toxin (Life Technologies, Inc.), 0.5 μg/ml hydrocortisone (Sigma), 10 μg/ml insulin (Sigma), 20 ng/ml epidermal growth factor (Sigma), and 5% horse serum (Life Technologies, Inc.). MDA-MB-231 cells (American Type Culture Collection), a human breast cancer cell line, were passaged into nude mice (mammary fat pad) and back out to *in vitro* culture for at least four cycles. The resulting variant cell line, which was enriched in the ability to grow in the fat pad and metastasize, was maintained in MEM α media (Life Technologies, Inc.) completed with 2.2 g/L of sodium bicarbonate, 1% HEPES, 1% L-glutamine, 10% heat-inactivated fetal bovine sera, 1 μg/ml of insulin, 1% sodium pyruvate, and 1% nonessential amino acids. For all studies, low passage (p) cells, between p5 and p15, were used.

Three-Dimensional Culture Model

MCF-12A or MDA-MB-231 cells were cultured in three-dimensional culture as previously described.[13] Briefly, log-phase cells were harvested and overlaid onto 2-mm-thick matrix pads at cell concentrations of 4.5×10^4 (MCF-12A) or 1.5×10^4 (MDA-MB-231) in a 96-well format (Sarstedt, Newton, NC). The matrix substratum was composed of 50 μl of nulliparous or involution rat mammary gland matrix (normalized for total protein concentration) mixed 1:1 with Matrigel (BD Biosciences, San Jose, CA). For these three-dimensional studies, Matrigel is required to facilitate polymerization of endogenous mammary matrix. For control conditions, the pad was composed of Matrigel without endogenous mammary matrix. For MCF-12A cells, 5% horse serum was added to the matrix pads. Three-dimensional culture assays were performed in triplicate and each experiment performed in duplicate with two different batches of endogenous mammary matrix. Organoids were photographed using an inverted microscope (Zeiss Axioscope 25) at 120 hours after plating.

Invasion Assays

Log-phase MDA-MB-231cells (5×10^4 cells) were suspended in 200 μg/ml of Matrigel, nulliparous, or involution mammary gland matrix and overlaid onto transwell 8-μm pore filters in 24-well plate format (Becton Dickinson, Mountain View, CA). In the lower chamber, 1.0% fetal bovine serum was used as a chemoattractant. The number of invasive cells, evaluated 24 hours after plating, was quantified as previously described.[15] Invasion assay was performed in triplicate and data are expressed as mean $\pm$ SEM. For the invasion assays designed to model the xenograft conditions, 2×10^6 cells mixed with 20 μl of matrix were injected onto the tops of transwell filters using 0.5% fetal bovine serum as a chemoattractant in the lower chamber and cell invasion and morphology determined after 24 hours.

Zymogen Assay

Substrate gel analyses were performed as described.[15] Briefly, ECM samples loaded as equal protein were electrophoresed under nonreducing conditions on a 7.5% sodium dodecyl sulfate-polyacrylamide gel containing 3 mg/ml of porcine gelatin (Sigma). Gels were incubated in a shaking water bath at 37°C for 72 hours in substrate buffer (50 mmol/L Tris-HCl, pH 8.0, 5 mmol/L $CaCl_2$). Proteinase activity was visualized by Coomassie Blue R250 staining. Zymogen activity appears as a cleared band in a dark background.

Xenograft Model

Forty-eight, 8-week-old female homozygous Nu/Nu athymic nude mice (NCI, Frederick, MD) were randomized by weight into three groups with 16 mice per group. The animals were anesthetized using isoflurane (Minrad, Inc., Bethlehem, PA). Log phase MDA-MB-231 cells were mixed with 300 μg/ml of Matrigel, nulliparous or involution mammary matrix at a concentration of 1.0×10^5 cells/μl matrix. Twenty μl of the cell/matrix mix (2×10^6 total

cells) were back-loaded into a 3/10-ml insulin syringe with a 29-gauge ½-inch needle (BD Biosciences, San Jose, CA) and injected into the fat pad of mammary gland no. 4, based on previously published methods.[24] Tumor growth was measured using calipers twice a week. Body weight measurements were taken at study end. At 72 hours, 2 weeks, and 4 weeks after injection, one animal per group was sacrificed and tumor histology analyzed. The remaining animals were sacrificed at 6 weeks after tumor cell injection. At study end, tumors with a small border of mammary gland tissue attached were excised and weighed, and final tumor weight and volume were calculated ($4/3\pi R^2h$). Liver, lung, kidney, and brain tissues were isolated. To minimize the possibility of cross contamination between tissues, fresh, sterile surgical tools were used for each tissue isolation. All tissues were rinsed in three changes of sterile phosphate-buffered saline to remove residual blood and possible tumor cell contamination. Half of all primary tumors and organs were flash-frozen in liquid nitrogen and stored at −80°C for molecular and biochemical analyses. The other half of the tumor and organs were fixed in 10% neutral-buffered formalin for 18 hours, paraffin-embedded, and processed for H&E and immunohistochemical staining.

RNA Analysis

RNA was isolated using the RNeasy mini kit according to the manufacturer's protocol (Qiagen, Valencia, CA). Reverse transcriptase (RT) reactions were performed with gene-specific reverse primers and 0.25 μg of total RNA. One μl of each RT reaction was used in a 50-μl polymerase chain reaction (PCR) reaction volume with 35 cycles. Standard curves were generated using human MDA-MB-231 RNA diluted in mouse mammary gland RNA to bring the final total RNA concentration to 0.25 μg. Data from the standard curve (not shown) indicates that we can detect as little as 25 pg of human RNA, or 1 human cell for every 10,000 mouse cells. Human-specific primers were developed to β2-microglobulin (β2M) (forward β2M: 5′-GGC TGG CAA CTT AGA G-3′; reverse β2M: 5′-GCC TTA CTT TAT CAA ATG TAT-3′). GAPDH was used as a loading control (forward GAPDH: 5′-GCC AAG TAT GAT GAC A-3′; reverse GAPDH: 5′-TAT TAT GGG GGT CTG-3′). Primers were purchased from Macromolecular Resources (Fort Collins, CO). For β2M detection in lung samples, PCR reactions were performed four independent times, and representative data are shown. For real-time PCR, RT reactions were performed using oligo-dT primer. Two μL of each RT reaction was used in a 25-μl volume for SYBR Green (Applied Biosystems, Foster City, CA) detection. β2M expression levels were normalized to actin controls. Forward β-actin: 5′-GCA ACG AGC GGT TCC G-3′; reverse β-actin: 5′-CCC AAG AAG GAA GGC TGG A-3′. Data were collected using sequence detection system software (Applied Biosystems) and analyzed by the Ct method.[25] Vascular endothelial growth factor (VEGF) analysis was performed with a TaqMan probe system using random primers for the RT reactions and human GAPDH as the internal control (Applied Biosystems, Foster City, CA). Forward VEGF: 5′-AAT GAC GAG GGC CTG GAG T-3′; reverse VEGF: 5′-TTG ATC CGC ATA ATC TGC ATG-3′; TaqMan probe VEGF: 5′-TGT GCC CAC TGA GGA GTC CAA CAT A-3′. All PCR reagents, unless otherwise specified, were purchased from Roche Pharmaceuticals (Nutley, NJ). VEGF quantization was performed by the University of Colorado Health Science Center Cancer Center PCR Core Laboratory.

Immunohistochemistry

Tissue samples were pretreated in 10 mmol/L sodium citrate at 90°C for 20 minutes. Smooth muscle actin (SMA clone 1A4, 1:200; Neomarkers, Fremont, CA) was detected in 5-μm sections according to published methods.[13] Vimentin (clone 9, 1:400; Sigma) was detected with a standard avidin-biotin complex-peroxidase method with 3,3′-diaminobenzidine as the chromogen.

In Situ *Hybridization*

Fluorescence *in situ* hybridization was performed on neutral-buffered formalin-fixed tissue sections, as described,[26] using the following conditions. The sections were incubated in 2× standard saline citrate at 75°C for 20 minutes (tumor) or 15 minutes (liver). Tissues were digested in proteinase K (InnoGenex, San Ramon, CA) at 45°C for 12 minutes (tumor) or 10 minutes (liver). Human-specific Cot-1 DNA probe labeled with SpectrumRed was generated in the University of Colorado Cancer Center Cytogenetics Core Laboratory. Hybridization was performed for 14 hours at 37°C. Nuclei were detected using Vectashield 4,6-diamidino-2-phenylindole (DAPI) (0.3 μg/μl) diluted in Vectamount mounting medium (Vector Laboratories, Burlingame, CA). Slides were visualized at ×1000 on a Zeiss Axioscope 2 Plus using Cytovision 3.6 software from Applied Imaging.

Results

To begin our studies investigating the role of physiological changes in mammary stroma on tumor cell behavior, endogenous mammary matrix was isolated from female rats with different reproductive histories. Sprague-Dawley rats were chosen for these studies because changes in rat mammary ECM due to reproductive stage have been characterized[13,27] and because sufficient quantities of endogenous mammary ECM required for the *in vitro* and *in vivo* functional studies can be obtained. For our studies, ECM isolated from mammary glands undergoing weaning-induced involution serves as the active, tissue-remodeling ECM (involution matrix), whereas ECM isolated from glands of nulliparous rats serves as the quiescent, nonremodeling ECM (nulliparous matrix). For the involution matrix, mammary glands were pooled from an equal number of rats at 4, 5, and 6 days after weaning. This window of mammary gland regression coincides with the proteinase-dependent phase of gland regression and is characterized by high MMP-2, MMP-3, and MMP-9 activ-

ity and increased serine proteinase urokinase-type plasminogen activator levels.[13,15,28] During this phase of involution, lobuloalveolar structures collapse and tissue remodeling is intensive.[28,29] We have previously shown that endogenous ECM isolated from rat mammary glands at this phase of involution has increased fibrillar collagen, proteolytic fragments of the matrix proteins laminin and fibronectin, and elevated MMP-2 and MMP-9 activity, whereas nulliparous matrix did not.[13,15,17,29] Consistent with our previous results, stroma histology and ECM isolated from pooled mammary glands of rats at 4, 5, and 6 days after weaning demonstrated these wound-healing attributes. As seen in Figure 1a, fibrillar collagen was detected at high levels in the interlobular stroma of involuting glands (Figure 1a). Further, in ECM isolated from these mammary glands, intact fibronectin and laminin, as well as fibronectin and laminin fragments, were detected at higher levels in involution matrix compared to nulliparous matrix (Figure 1b). Consistent with the ECM proteolysis detected by Western blot, MMP-9 and MMP-2 activities were elevated in involution matrix (Figure 1c).

Having demonstrated biochemical differences in ECM isolated from quiescent and involuting glands, we next assessed whether these matrices differ functionally in their ability to influence mammosphere development in three-dimensional culture. To evaluate mammary ECM effects on normal mammary epithelial cells, we used MCF-12A cells, an immortalized but nontransformed human mammary epithelial cell line.[23] We have previously demonstrated that MCF-12A cells form hollow, alveoli-like mammospheres when overlaid onto thick Matrigel pads.[30] MCF-12A cells were overlaid onto matrix pads containing nulliparous matrix, involution matrix, or Matrigel. MCF-12A cells overlaid onto Matrigel formed simple spherical mammospheres (Figure 2a, i). In contrast, MCF-12A cells overlaid onto nulliparous matrix formed duct-like structures with complex branching (Figure 2a, ii). Similar to cells overlaid onto Matrigel, MCF-12A cells plated onto involution matrix failed to organize into duct-like structures and instead formed simple spherical mammospheres (Figure 2a, iii). In all cases, the MCF-12A mammospheres were hollow in the center, forming small alveoli-like structures, with histology consistent with their nontransformed phenotype (Figure 2a, iv). These data demonstrate that nulliparous and involution matrix differ functionally because nulliparous matrix contained organizing signals for duct-like development whereas involution matrix and Matrigel did not.

We next evaluated the effects of these matrices on three-dimensional organization of MDA-MB-231 cells, a highly tumorigenic human breast cancer cell line. MDA-MB-231 cells did not form alveoli-like mammospheres on

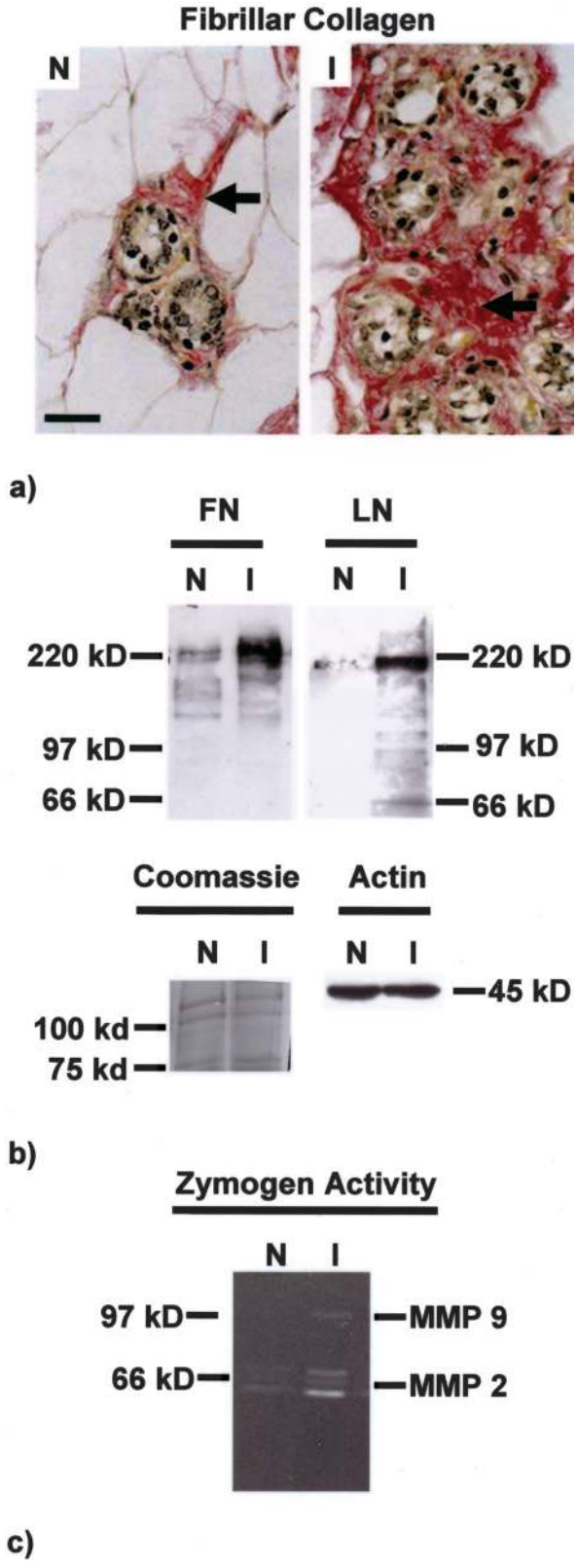

Figure 1. Involution matrix shows attributes of provisional wound-healing stroma. **a:** Fibrillar collagen deposition is increased in the mammary glands of female rats undergoing weaning-induced involution (I) compared to nulliparous rats (N). Fibrillar collagen was detected histologically on 5-μm sections using Sirius Red F3Ba and Weigert's iron hematoxylin counterstain. **Arrows** point to red-staining interlobular fibrillar collagen. **b:** Fibronectin (FN) and laminin (LN) levels are increased in involution matrix (I) compared to nulliparous matrix (N), as shown by Western blotting of mammary matrix preparations loaded by equal protein. A Coomassie Blue-stained gel is shown to demonstrate equal protein lane loading, and tissue actin is shown to demonstrate equal cellular content of the starting material from which the mammary matrix was extracted. **c:** MMP-2 and MMP-9 zymogen activities are enhanced in involution matrix (I) compared to nulliparous matrix (N). Matrix loaded by equal protein. Scale bar, 50 μm.

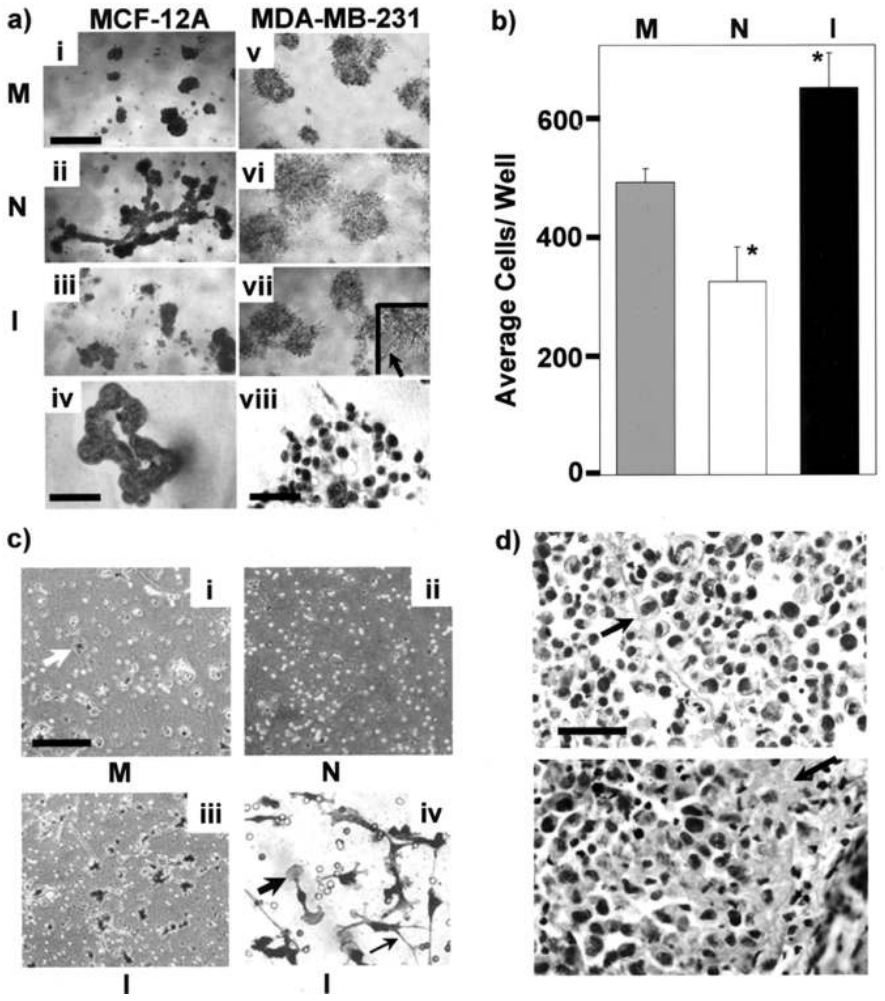

Figure 2. Quiescent and involution matrix differentially promote mammary epithelial cell organization and invasion. **a:** In three-dimensional culture assays, nontransformed human mammary epithelial MCF-12A cells form simple spheroid mammospheres on Matrigel (**i**), organize into duct-like structures with complex branching on nulliparous matrix (**ii**), and form simple mammospheres on involution matrix (**iii**). H&E-stained 5-μm section of MCF-12A organoid on nulliparous matrix shows highly organized duct-like structure with hollow central lumen (**iv**). MDA-MB-231 cells, derived from a highly aggressive human breast cancer, did not form mammospheres on any matrix and instead formed loosely organized clusters of cells (**v**, **vi**, **vii**) with invasive filopodia, as seen in the **inset** of **vi**. H&E-stained 5-μm section of a MDA-MB-231 organoid shows that these cells lack lateral adhesion junctions and are not hollow. **b:** In a transwell filter invasion assay, involution matrix (I) promoted MDA-MB-231 cell invasion more than either nulliparous matrix (N) or Matrigel (M). *Statistically significant difference between N and I; $P = 0.010$ (paired *t*-test). **c:** In an invasion assay modeling xenograft conditions (2×10^6 cells in 20 μl of matrix), involution matrix preferentially promoted cell invasion. **i:** Matrigel/tumor cell bolus (M), and **ii:** nulliparous matrix/tumor cell bolus (N). The transwell filter pores appear as **white circles**, and the invasive cells stain purple (**white arrow**). In **iii**, more cells invaded in response to being precoated with involution matrix (I). **iv:** Involution matrix (I)-treated cells had lamellopodia (**thick arrow**) and filopodia (**thin arrow**). **d:** Physical interaction between the tumor cells and endogenous matrix in the xenograft model was confirmed by removal of ECM/tumor cell inoculates 72 hours after injection. The **top** panel shows representative image of cells adhered to matrix fibrils present in involution matrix (**arrow**) and nulliparous matrix (data not shown). Matrigel lacks a fibrillar component and thus did not show this type of cell-fibrillar matrix interaction. In the **bottom** panel, tumor cells are enveloped in nulliparous matrix (**arrow**), which is representative of all groups. Scale bars: 100 μm [**a** (**i–iii**, **v–vii**)]; 50 μm [**a** (**iv**, **viii**), **c** (**i–iii**), **d**]. Original magnifications: ×50 [**a** (**i–iii**, **v–vii**), **c** (**i–iii**)]; ×200 [**a** (**iv**, **viii**), **c**, **iv**]; ×400 [**a**, **vii** (inset), **d**].

any matrix (Figure 2a, v, vi, and vii). When these three-dimensional tumor cell organoids were sectioned, hollow lumens were absent (Figure 2a, viii), a phenotype consistent with their aggressive tumor-forming ability.[4] Further, MDA-MB-231 cells were locally invasive in all matrices as evident by numerous filopodia invading the surrounding stroma (Figure 2a, vii, inset, and viii). These observations demonstrate that in this three-dimensional culture assay, nontumorigenic and tumorigenic cell lines vary dramatically in their response to isolated endogenous mammary gland ECM.

The ability of the mammary matrices to influence mammary epithelial cell motility and invasiveness was determined next using transwell filter assays, in which cells are overlaid onto the respective matrices and allowed to respond to a chemotactic signal. Consistent with their nontransformed phenotype, MCF-12A cells were nonmotile and noninvasive (data not shown). Conversely, MDA-MB-231 cells were uniformly and highly motile on all three matrices tested (data not shown). In contrast to the motility results, invasion of MDA-MB-231 cells in transwell filter assays was found to be dependent on the source of matrix, with invasion highest when cells were in contact with involution matrix (Figure 2b). To model the ECM/tumor cell interactions present in the xenograft model, a second transwell filter invasion assay was performed. For this assay, tumor cells were mixed with matrix and the tumor cell/ECM bolus placed onto the tops of the trans-

well filters. The ability of the tumor cells to migrate out of the ECM and traverse the filter was evaluated. Cell migration out of the Matrigel and nulliparous matrix was very low (Figure 2c, i and ii), whereas involution matrix promoted some tumor cell invasion (Figure 2c, iii). Further, involution matrix induced lamellopodia and filopodia formation, cellular processes consistent with motility and invasiveness (Figure 2c, iv; arrows).

Orthotopic Xenograft Model for Breast Cancer Metastasis

Based on the demonstration that involution matrix promotes tumor cell invasion *in vitro*, we investigated whether involution matrix increases metastasis *in vivo*. For this study, MDA-MB-231 cells were mixed with matrix and injected into the inguinal fat pads of female nude mice. We first sought to determine the physical interaction between the tumor cells and the matrix after injection into the mouse mammary fat pad. For these experiments, the tumor cell/ECM inoculates were removed 3 days after injection and processed for histological evaluation. We found that the human tumor cells interacted strongly with the rat mammary matrix. Within the ECM inoculates, tumor cells adhered to rat mammary gland matrix fibrils (Figure 2d, upper panel arrow) and were enveloped by matrix (Figure 2d, lower panel arrow). Matrix fibrils with tumor cells attached were found in the nulliparous and involution matrix inoculates but not in the Matrigel inoculates (data not shown), most likely because Matrigel lacks a fibrillar component. The influence of the various ECM matrices on tumor cell death was also evaluated, and cell death was found to be minimal and to not differ between groups (data not shown). In the 13 mice/group remaining, tumor growth was measured twice weekly throughout the course of the 45-day study. Primary tumor growth rates and final tumor volumes were identical in the nulliparous matrix and involution matrix groups (Figure 3a and Table 1). Tumor growth in the Matrigel group was slightly suppressed, but this difference did not reach statistical significance. We next investigated whether the source of matrix influenced the ability of tumor cells to metastasize from the mammary fat pad to distant organs.

Detection of Metastatic Lesions

The presence of human tumor cells in mouse lung tissue was detected by two complimentary methods. Human tumor cells present in mouse lung tissue were identified by immunohistochemical detection of vimentin, a cytokeratin expressed in the aggressive epithelial tumor cell line MDA-MB-231 but not in normal mammary or lung epithelium. In a mammary fat pad tumor from the involution group (Figure 3b, left), vimentin-positive, brown-staining MDA-MB-231 cells within the mouse mammary fat pad were readily apparent, whereas the mouse mammary epithelial cells lining the mammary ducts were vimentin-negative (Figure 3b, left, asterisk). Vimentin-positive human tumor cells were also present within the mouse lung (Figure 3b, right; arrows). The second detection method used was RT-PCR of human RNA in mouse lung tissue using human-specific primers to β2M. There is a correlation in results between the two methods used to detect metastases (Figure 3c, data from Matrigel group shown). Further, we found that the probability of a mammary tumor to metastasize to the lung was signif-

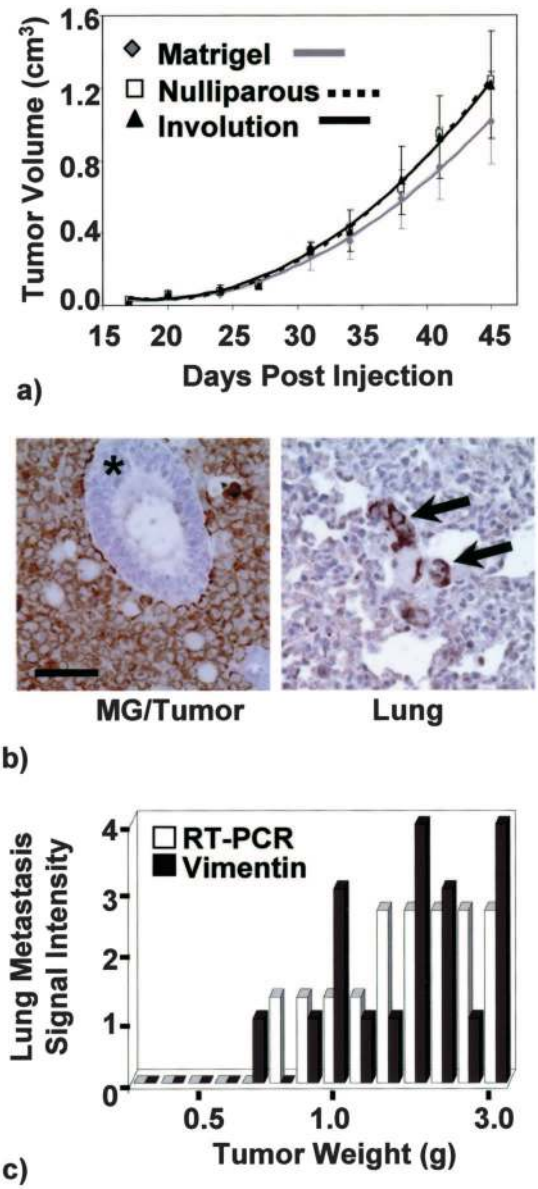

Figure 3. Tumor growth and detection of metastasis. **a:** Tumor volumes of mammary fat pad tumors were calculated twice weekly. Nulliparous and involution matrix group tumor growth was identical. Matrigel group tumors were slightly smaller; however, this difference did not reach statistical significance. **b:** Tumor cell-specific vimentin was detected by immunohistochemistry. **Left**: Mouse mammary fat pad with human tumor cells positive for vimentin and normal mouse ductal epithelial cells (**asterisk**) negative for vimentin. **Right**: Vimentin-positive tumor cells, depicted by **arrows**, in the lung of an involution matrix group animal. **c:** Graph showing relationship between the size of primary tumor and likelihood of lung metastasis in individual animals, as determined by immunohistochemical detection of vimentin-positive cells and RT-PCR detection of human RNA using human-specific primers to β2M. There was a strong correlation between detection of metastases in lung and size of the primary tumor (data for Matrigel shown). For these analyses, RT-PCR and immunohistochemical signal intensities were divided into quartiles. Scale bar, 50 μm (**b**). Original magnifications, $\times$400 (**b**).

Table 1. In the Xenograft Study, Average Body Weights and Mammary Tumor Volumes Did Not Differ between Groups

	Final body weight (g)	Final tumor volume (cm^3)
Matrigel	25.8 ± 0.46	1.02 ± 0.25
Nulliparous	25.6 ± 0.54	1.18 ± 0.05
Involution	24.7 ± 0.63	1.09 ± 0.30

Column one lists the average final body weights of animals in the Matrigel, nulliparous, and involution groups with their standard deviations. There is no difference between the groups. Column two shows average final tumor volumes and their standard deviations for Matrigel, nulliparous, and involution groups. Tumor dimensions were measured with calipers and volumes calculated with the formula $V = 4/3\pi R^2 h$. There is not a statistically significant difference between the groups.

icantly influenced by the size of the primary tumor. In our model, once a tumor attained a mass of 1 g, it metastasized independent of the source of matrix at time of tumor cell injection. Therefore, to address the question of whether the source of matrix influenced metastatic rate, we focused our analysis on mice that had small (1 g or less) mammary fat pad tumors.

Involution Matrix Promotes Metastasis

The ability of small tumors to metastasize out of the mammary fat pad was found to be highly dependent on the source of matrix. In the involution group, more than twice as many mice (six of nine) had metastatic lesions in their lungs than mice in the nulliparous matrix (two of seven) or Matrigel groups (two of eight) (Figure 4a). To confirm and extend this investigation, metastatic lesions in lung, liver, kidney, and brain were identified by quantitative PCR. Consistent with the lung metastasis data, quantitative PCR analyses confirmed that lung metastatic lesions were more frequent in mice in which tumor cells had been mixed with involution matrix before fat pad injection (Figure 4b). Similarly, metastatic events to liver and kidney were higher in the involution matrix group (Figure 4b). Metastatic lesions in brain were rare in all groups.

In situ hybridization, using a human-specific Cot-1 DNA probe, was used to confirm that the human-specific PCR signals detected in the liver were in fact due to metastasis of human tumor cells from the mammary fat pad to the liver. By this method, human tumor cells within the mouse mammary fat pad are evident (Figure 4c, i; asterisk), as is migration of the tumor cells into the surrounding mouse fat pad (Figure 4c, i; arrow). Further, clusters of human mammary tumor cells could be detected in the mouse liver sections (Figure 4c, ii), corroborating the quantitative RT-PCR analyses.

We next investigated potential pathways by which tumor cells disseminated from the mammary gland. In some mice with metastatic lesions in the lungs, metastases to mammary lymph nodes were identified (Figure 5a, i). In our study, the number of lymph node metastases detected was too small to analyze statistically. An alternative route by which tumor cells might escape from the mammary gland is through the blood vessels. We found that tumors from the involution group had increased vascular density at the tumor/mammary gland border, indicating the induction of angiogenesis. Further, the apparent induction of angiogenesis in the involution group was a very early event. As early as 72 hours after tumor cell injection, an angiogenic response was evident as measured by an increase in microvessel density (Figure 5a, ii; arrow) and by the presence of vessels with increased diameter (data not shown). This increase in vasculature at the tumor/mammary gland border was evident in the involution group at all time points evaluated: 72 hours, 2 and 4 weeks (data not shown), and 6 weeks after injection. At study end, vasculature at the tumor/mammary gland border was more prominent in the involution group (Figure 5a, v), compared to the nulliparous and Matrigel groups (Figure 5a, iii and iv). Of note, the tumor vasculature did not develop uniformly around the tumors but rather developed focally. Similarly, evidence for reactive stroma, as measured by smooth muscle actin expression in host fibroblast cells, was also focally induced more frequently in the involution group compared to the nulliparous group (Figure 5b, top and bottom, respectively). In an attempt to quantify the angiogenic response between groups, the levels of VEGF produced by the tumors were determined by quantitative RT-PCR. Human-specific VEGF primers and probes were used to detect only VEGF produced by the human tumor cells. VEGF levels were statistically higher in the tumors obtained from the involution group in comparison to the nulliparous and Matrigel group tumors (Figure 5c, left). Because we demonstrated that primary tumor size correlated positively with metastatic ability (Figure 3c), we verified that the elevated VEGF expression in the involution group tumors was not due to higher tumor burden in this group. When VEGF levels were normalized to tumor size, the levels of VEGF were more than twofold higher in the involution group compared to the nulliparous and Matrigel group tumors (Figure 5c, right). Therefore, involution matrix may stimulate MDA-MB-231 cells to secrete VEGF.

Discussion

During weaning-induced mammary gland involution, milk-secreting epithelial cells are eliminated, and the gland regresses to a quiescent organ that is composed predominantly of a denuded mammary epithelial tree embedded in an adipose-rich stroma. This regression process is characterized by dramatic tissue remodeling and massive cell death of the milk-secreting epithelium.[29,31] In contrast to the tissue damage and necrosis typically associated with wound-healing and inflammation-induced tissue remodeling, mammary gland involution is an orderly, programmed, physiological cell death process. As such, mammary gland involution has been regarded as a noninflammatory, tissue-remodeling process.[32] However, the role inflammation plays during involution has been reassessed recently. This is, in part, because detailed transcript analyses during weaning-induced involution have identified evidence for a wound-healing response.[16,33] Within the involuting gland, molec-

ular markers for both innate and adaptive immunity have been identified, providing evidence for neutrophil, macrophage, T-cell and B-cell activation.[16,33] This new microarray data corroborates studies that characterized cell types and stromal proteins present within the actively involuting gland, and which identified many similarities between involution stroma and provisional wound-healing stroma. These comparisons include infiltration of neutrophils, macrophages, and plasma cells;[27,33,34] elevated matrix metalloproteinase activity;[17,18] high levels of fibrillar collagen;[13] and proteolytic fragments of laminin[13,19] and fibronectin.[13,17] The presence of fibronectin proteolytic fragments during gland involution is of particular relevance because fibronectin fragments have been demonstrated to activate MMP-9 during wound healing and reinforce the tissue-remodeling process.[35] Hence, physiological tissue remodeling of the mammary gland appears to use some of the same programs activated during wound healing and inflammation.[17]

In addition to sharing biochemical similarities with wound-healing stroma, involution stroma shares functional similarities. For example, wound-healing stroma eliminates damaged epithelium from the wound site. The process of involution also eliminates unwanted epithelial cells from the mammary gland, and involution matrix can induce death of immortalized, but nontransformed mammary epithelial cells in culture.[13,17] Another attribute of wound-healing stroma is to stimulate mesenchymal cell synthetic activity, motility, and invasiveness, processes that facilitate wound closure and remodeling of damaged tissue. Importantly, like mesenchymal cells, tumor cells can also be activated by wound-healing stroma, resulting in increased synthetic activity, motility, and invasiveness.[1–6] Similar to the effects that wound-healing stroma can have on tumor cells, we have found that involution matrix activates human mammary tumor cell motility and invasion *in vitro*.[15] Here, we extend these studies to investigate whether involution matrix promotes metastasis of tumor cells in a xenograft model for human breast cancer. We found that human breast cancer MDA-MB-231 cells metastasized to lung, liver, and kidney at significantly increased rates when the tumor cells were mixed with involution matrix compared with tumor cells mixed with nulliparous matrix or Matrigel. The increase in metastasis correlated with a twofold increase in VEGF expression in the involution group tumors. Moreover, the involution group tumors were more likely to exhibit angio-

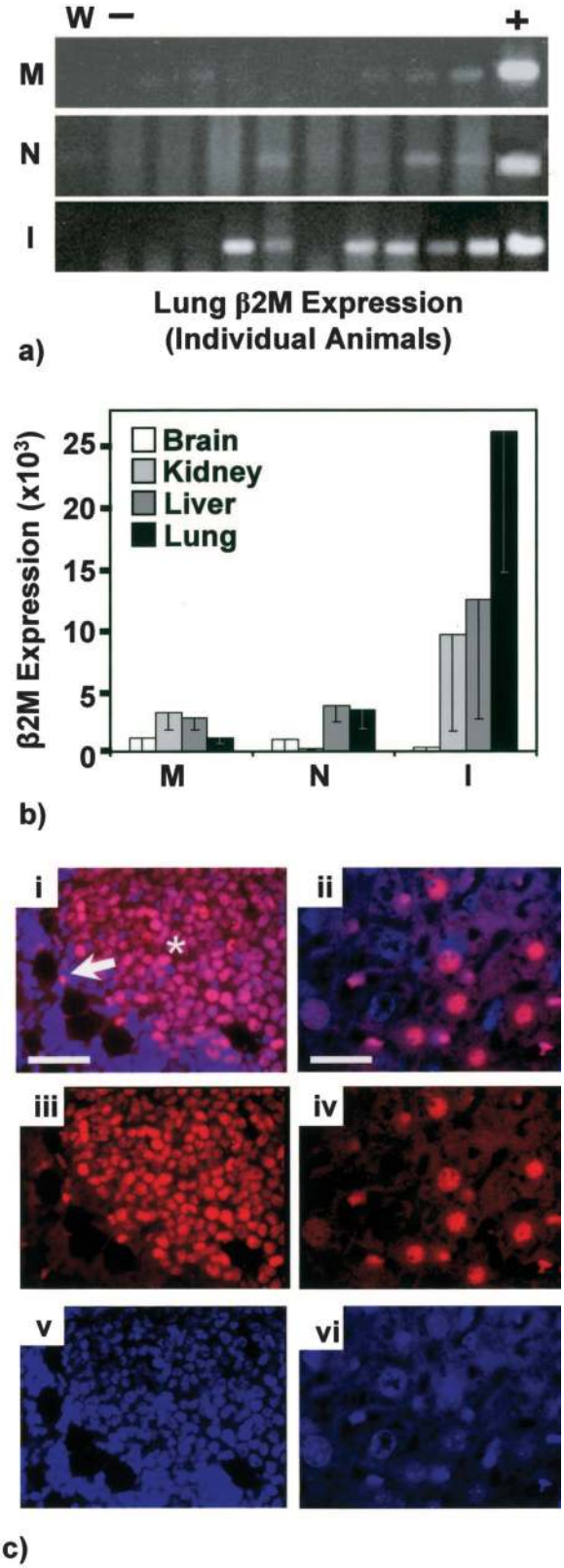

Figure 4. Involution matrix preferentially promotes metastasis to lung, liver, and kidney. **a:** In mice with mammary fat pad tumors less than 1 g, metastasis to lung was detected by RT-PCR using human-specific primers to β2M. Involution-group mice had more than twice the incidence of metastasis to lung. Each lane depicts signal from lung tissue of one animal. W, water control lane; −, negative control lane of mouse RNA only; and +, positive control lane of MDA-MB-231 cell RNA. M, Matrigel group mice; N, nulliparous group mice; and I, involution group mice. **b:** Real-time SYBR Green PCR on brain, kidney, liver, and lung RNA using human-specific primers to β2M with expression signal normalized to mouse β-actin. Involution group animals had more frequent metastasis to lung, liver, and kidney. Brain metastases were rare in all groups. **c:** Human Cot-1 DNA probe, labeled with Spectrum Red, was used to detect human tumor cells in mouse tissue. **i:** Dual image of red fluorescent human tumor cells and DAPI-stained nuclei at the tumor/mammary gland border from an involution group animal. **Asterisk** depicts tumor and **arrow** points to a tumor cell that has invaded the mammary fat pad. **ii:** Dual image of red fluorescent human tumor cells and DAPI-stained nuclei in the liver of the same animal. **iii** and **iv:** Only the signal from the human tumor cells are shown whereas **v** and **vi** show only the DAPI signal in mammary gland and liver, respectively. Scale bars: 60 μm (**c**, **i**, **iii**, and **v**); 20 μm (**c**, **ii**, **iv**, and **vi**).

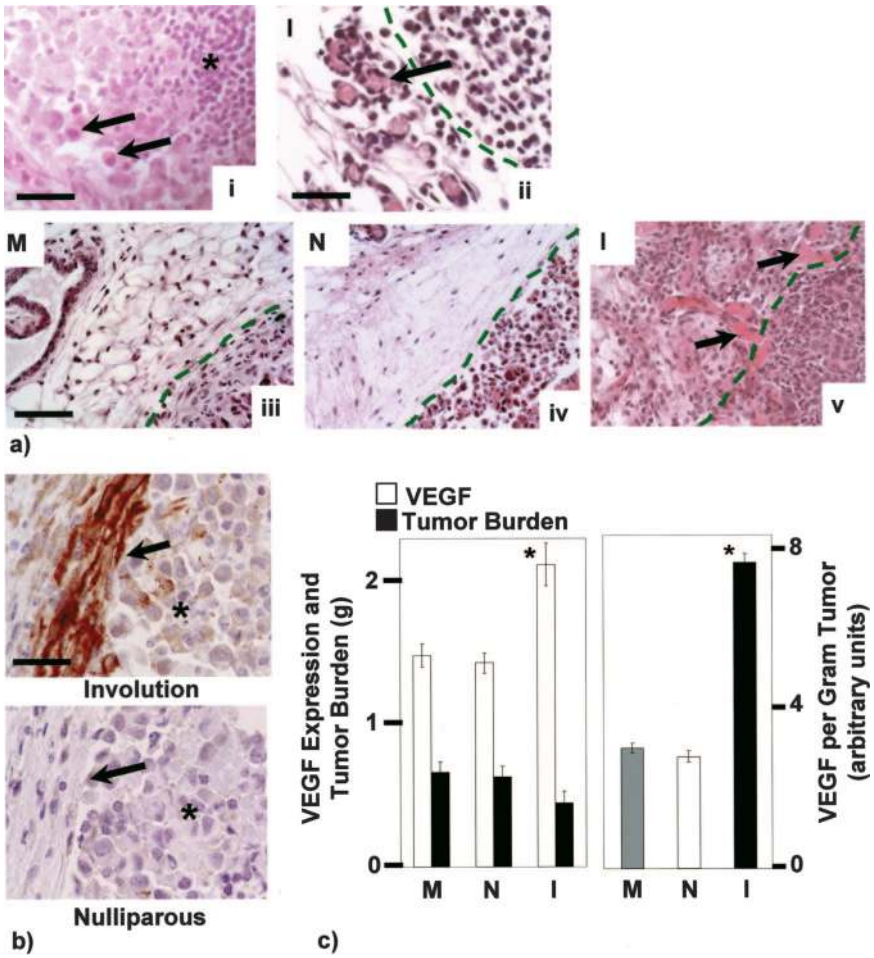

Figure 5. Involution matrix promotes angiogenesis, fibroblast activation, and VEGF expression. To evaluate paths of metastasis, metastasis to mammary lymph nodes and vascularization at the tumor/mammary gland border were analyzed. **a: i:** Metastatic human MDA-MB-231 cells (**arrows**) in a mammary lymph node (**asterisk** depicts lymph cells within node). **ii:** Neovascularization at the tumor/mammary gland border in an involution group animal (I) at 72 hours after tumor cell injection. The border between the mammary gland and tumor bolus is depicted with **green hatch marks**. Numerous small vessels are evident at the border of the tumor bolus (**arrow**). At 6 weeks, focal angiogenic response was infrequent at the border of Matrigel group (**iii**) and nulliparous group tumors (**iv**) but was common in involution group tumors (**v**, **arrows**). Tumor/mammary gland borders shown are representative. **b:** Smooth muscle actin, a marker of reactive stroma, is present in fibroblasts in a representative involution group tumor (**top**) but is absent from the nulliparous group tumor stroma (**bottom**). The **arrows** show the tumor stroma border, **asterisks** depict tumor. **c:** Human tumor VEGF expression as a marker for angiogenesis was measured by quantitative real-time PCR. The average relative VEGF expression values, normalized to GAPDH expression levels, are reported for each group (**open bars**, **left**). The average tumor burden (g) per group is also shown (**filled bars**, **left**). VEGF expression in the involution group is statistically different from both nulliparous and Matrigel groups (Bonferroni *P* values: I versus M, $P = 0.01$; I versus N, $P < 0.0001$; M versus N, $P = 0.15$). In the **right graph**, VEGF expression levels normalized to tumor burden are shown (arbitrary units). Scale bars: 50 μm (**a**, **i**, and **ii**); 100 μm (**a**, **iii**, **iv** and **v**); 40 μm (**b**).

genesis and have reactive stroma (desmoplastic stroma) characteristics at the border between the tumor and the host mammary gland. These data support the hypothesis that during mammary gland involution, the tissue microenvironment is better able to promote tumor cell dissemination by increasing tumor cell motility, invasiveness, VEGF expression, and desmoplastic stroma. In support of this hypothesis, it has been shown in mammary glands of mice overexpressing activated stromelysin 1 that there is a progressive development of reactive stroma, an involution-phenotype, and formation of mammary epithelial tumors.[36,37] Further, this is the first study to demonstrate that ECM isolated from physiologically normal mammary glands can influence metastatic tumor cell behavior *in vivo*.

Our observation that a small amount of matrix at time of tumor cell injection can have profound effects on subsequent tumor development is not unprecedented. Tumor cells premixed with Matrigel before injection in xenograft models have been demonstrated to permit tumor development of otherwise nontumor-forming cells, including small cell lung cancer and melanoma cells, as well as primary renal and breast carcinomas.[24,38,39] Further, there is evidence that tumor formation and subsequent metastasis does not require the continued presence of the matrix. Rather, it appears as if the matrix initiates altered programs of tumorigenesis early on, and these programs persist as the tumor grows.[40,41] Thus, a small amount of matrix at the time of tumor cell injection can, in fact, have profound and persistent effects on the tumor cell phenotype, presumably through an epigenetic mechanism. Of note, in our study, the metastatic events occurred early and frequently in the involution group, and thus it is unlikely that the promotional effect of matrix on

metastasis was due to newly acquired mutations in the tumor cell genomes.

The observation that mammary tumors from the involution group were more vascularized at the tumor mammary gland border than tumors from the nulliparous or Matrigel groups raises the question of whether involution matrix contains high levels of proangiogenic factors. During weaning-induced involution, the vasculature that supports the lactating gland regresses concurrent with the secretory epithelium.[27] Therefore, it is plausible that involution tissue would have elevated levels of anti-angiogenic proteins.[42,43] To complicate matters, concurrent with regression of the secretory epithelium and its blood supply is the re-establishment of the mammary fat pad blood supply.[44] The question of whether involution matrix contains proangiogenic factors remains to be determined. However, our data suggests that contact of tumor cells with involution matrix results in secretion of proangiogenic factors by the tumor cells. As early as 72 hours after tumor cell injection, abnormally large vessels and new angiogenic sprouts were detected at the boundary between the mammary fat pad and the involution group tumor cells, indicating that local endothelial cells respond early and dramatically to tumor cells mixed with involution matrix. Second, tumors in the involution group expressed the highest levels of VEGF, a potent inducer of angiogenesis.[45] VEGF secretion by the tumor cells may account for both the neovascularization and for the presence of the abnormally large blood vessels. Nagy and colleagues[45] and Pettersson and colleagues[46] have demonstrated that early after tissue treatment with VEGF, greatly enlarged, thin-walled vessels called mother vessels develop from pre-existing microvessels due to the release of cytoplasmic stores of plasma membrane-rich microvesicles.

In addition to the apparent mother vessel formation and neovascularization occurring at the tumor mammary gland border of involution group tumors, we observed focal activation of fibroblasts. With activation, fibroblasts express smooth muscle actin and become motile, which is a hallmark of reactive stroma.[47] Platelet-derived growth factor is one tumor-derived factor that has been shown to induce reactive stroma in a xenograft model for human breast cancer.[48] Platelet-derived growth factor is also a potent proangiogenic factor. The question of whether involution matrix up-regulates platelet-derived growth factor in mammary tumor cells is under investigation.

The *in vivo* study reported here raises the question of whether regression of the mammary gland after weaning promotes breast cancer progression. This question may be of particular importance for women who are diagnosed with pregnancy-associated breast cancer, defined as breast cancer occurring within 5 years of pregnancy. Based on our results, we hypothesize that a subset of women, those with occult disease at the time of pregnancy, are at increased risk for tumor cell dissemination during regression of the mammary gland after pregnancy.[5] This hypothesis appears in conflict with the demonstrable protective effect of pregnancy. However, the protective effect of pregnancy is neither immediate nor constant. Early first-term and multiple full-term pregnancies are associated with a lifetime reduction in risk for breast cancer in women.[49] In contrast, first full-term pregnancy in older women has been associated with a permanent increase in breast cancer risk.[49] Further, even first pregnancy at a young age is associated with a transient but significant increase in breast cancer risk.[49–51]

In addition, and of potential relevance to our work, women with pregnancy-associated breast cancer have a significantly poorer prognosis because of higher incidence of metastatic disease.[52,53] Because pregnancy is characterized by elevated levels of estrogen and progesterone, hormones intimately associated with breast cancer etiology and progression,[54,55] elevated levels of the gestational hormones have been hypothesized to be responsible for the poor prognosis of pregnancy-associated breast cancer.[54] Specifically, estrogen and progesterone are anticipated to increase risk and negatively affect prognosis by virtue of their growth-promoting effects on hormone-responsive breast tumor cells. However, data to support this hypothesis are inconsistent.[56] First, pregnancy at time of diagnosis has not been demonstrated to be an independent prognostic factor, indicating that factors other than the growth-promoting effects of gestational hormones are primarily responsible for poor prognosis of pregnancy-associated breast cancer.[56] Second, diagnosis of breast cancer in the first years after childbirth is an independent negative prognostic factor.[56] Further, the negative effect of a recent pregnancy on prognosis appears to persist even after adjustments are made for age of mother, tumor size, stage, histological grade, mitotic index, and ER, PR, Her2/neu, and p53 status.[53,56,57] These observations suggest that the poor prognosis of pregnancy-associated breast cancer is not exclusively due to the cell proliferative effects of the pregnancy hormones. We hypothesize that the reactive stroma-like microenvironment that accompanies regression of the mammary gland to its prepregnant state increases risk for tumor cell dissemination by activating a metastatic program in tumor cells. Thus, this developmental window, characterized by tissue remodeling, may account for the high mortality associated with breast cancer diagnosed after pregnancy.

It is important to note that there are several limitations to our study design. The xenograft model used, in which mammary gland ECM isolated from rats with distinct reproductive history is premixed with human breast tumor cells, probably models only a portion of the interactions between the tumor cell and its microenvironment. Specifically, the biochemical isolation of the mammary matrix may disrupt tissue architectural relationships that are important in determining metastatic efficiency. Further, important interactions between human mammary matrix and human tumor cells may be missing from our heterotypic studies. However, despite these limitations, one benefit of our study design is that we can identify effects due to the ECM component. Another limitation is that we have evaluated a single metastatic human breast cancer cell line, the MDA-MB-231 line. MDA-MB-231 cells display a poor-prognosis gene expression signature,[58] a signature profile originally identified by microarray anal-

yses of human breast cancers.[59] Thus, based on gene expression profiling, this commonly studied breast cancer cell line retains the molecular signature of aggressive human breast tumors and suggests that clinically relevant data can be obtained from the use of these cells.[58] Finally, we have isolated ECM from mammary glands forced to undergo involution by withdrawal of nursing pups. Gland involution induced by pup withdrawal has some known differences to that which occurs after natural weaning, including the rapid loss of IGF-1R and Akt protein.[60] It is unclear whether these differences might also be reflected in the ECM that relate to the phenotype described in this study.

In summary, we have demonstrated that the mammary gland microenvironment during weaning-induced regression has compositional similarities with provisional wound-healing stroma, specifically, elevated matrix metalloproteinase activity, high levels of fibrillar collagen, and proteolytic fragments of laminin and fibronectin. Using isolated endogenous mammary ECM as substratum for tumor cell invasion *in vitro* and to provide a tumor microenvironment in a xenograft model for breast cancer, we found that involution matrix promotes tumor cell invasion and metastasis, whereas mammary matrix isolated from quiescent mammary glands of nulliparous rats does not. These observations support previous work from our laboratory demonstrating that the microenvironment of the normal adult mammary gland is highly plastic because it is modified by systemic factors such as circulating hormones.[13,15] Based on data presented here, we propose that physiological changes in mammary ECM composition contribute to mammary carcinogenesis. Specifically, our data support the hypothesis that during mammary gland involution, the tissue microenvironment becomes promotional for tumor cell dissemination, providing a plausible mechanism to explain the high rate of metastases that occur with pregnancy-associated breast cancer.

Acknowledgments

We thank Steve Anderson and Heide Ford for critical review of the manuscript; Marileila Varella Garcia of the University of Colorado Health Science Center Cancer Center Cytogenetics Core and Umarani Pugazhenthi of the University of Colorado Health Science Center Cancer Center PCR Core for technical assistance; Hayley Ross and Luke Schnell for help with immunohistochemistry; and Dr. Pam Wolfe for statistical analyses.

References

1. Coussens LM, Werb Z: Inflammation and cancer. Nature 2002, 420:860–867
2. Bissell MJ, Labarge MA: Context, tissue plasticity, and cancer: are tumor stem cells also regulated by the microenvironment? Cancer Cell 2005, 7:17–23
3. Bissell MJ, Radisky D: Putting tumours in context. Nat Rev Cancer 2001, 1:46–54
4. Park CC, Bissell MJ, Barcellos-Hoff MH: The influence of the microenvironment on the malignant phenotype. Mol Med Today 2000, 6:324–329
5. Schedin P, Elias A: Multistep tumorigenesis and the microenvironment. Breast Cancer Res 2004, 6:93–101
6. Mueller MM, Fusenig NE: Friends or foes—bipolar effects of the tumour stroma in cancer. Nat Rev Cancer 2004, 4:839–849
7. De Marzo AM, DeWeese TL, Platz EA, Meeker AK, Nakayama M, Epstein JI, Isaacs WB, Nelson WG: Pathological and molecular mechanisms of prostate carcinogenesis: implications for diagnosis, detection, prevention, and treatment. J Cell Biochem 2004, 91:459–477
8. Shishodia S, Aggarwal BB: Cyclooxygenase (COX)-2 inhibitor celecoxib abrogates activation of cigarette smoke-induced nuclear factor (NF)-kappaB by suppressing activation of IkappaBalpha kinase in human non-small cell lung carcinoma: correlation with suppression of cyclin D1, COX-2, and matrix metalloproteinase-9. Cancer Res 2004, 64:5004–5012
9. Martins-Green M, Boudreau N, Bissell MJ: Inflammation is responsible for the development of wound-induced tumors in chickens infected with Rous sarcoma virus. Cancer Res 1994, 54:4334–4341
10. Barcellos-Hoff MH, Ravani SA: Irradiated mammary gland stroma promotes the expression of tumorigenic potential by unirradiated epithelial cells. Cancer Res 2000, 60:1254–1260
11. Kuperwasser C, Chavarria T, Wu M, Magrane G, Gray JW, Carey L, Richardson A, Weinberg RA: Reconstruction of functionally normal and malignant human breast tissues in mice. Proc Natl Acad Sci USA 2004, 101:4966–4971
12. Maffini MV, Soto AM, Calabro JM, Ucci AA, Sonnenschein C: The stroma as a crucial target in rat mammary gland carcinogenesis. J Cell Sci 2004, 117:1495–1502
13. Schedin P, Mitrenga T, McDaniel S, Kaeck M: Mammary ECM composition and function are altered by reproductive state. Mol Carcinog 2004, 41:207–220
14. Haslam SZ, Woodward TL: Reciprocal regulation of extracellular matrix proteins and ovarian steroid activity in the mammary gland. Breast Cancer Res 2001, 3:365–372
15. Bemis LT, Schedin P: Reproductive state of rat mammary gland stroma modulates human breast cancer cell migration and invasion. Cancer Res 2000, 60:3414–3418
16. Clarkson RW, Wayland MT, Lee J, Freeman T, Watson CJ: Gene expression profiling of mammary gland development reveals putative roles for death receptors and immune mediators in post-lactational regression. Breast Cancer Res 2004, 6:R92–R109
17. Schedin P, Strange R, Mitrenga T, Wolfe P, Kaeck M: Fibronectin fragments induce MMP activity in mouse mammary epithelial cells: evidence for a role in mammary tissue remodeling. J Cell Sci 2000, 113:795–806
18. Talhouk RS, Bissell MJ, Werb Z: Coordinated expression of extracellular matrix-degrading proteinases and their inhibitors regulates mammary epithelial function during involution. J Cell Biol 1992, 118:1271–1282
19. Giannelli G, Pozzi A, Stetler-Stevenson WG, Gardner HA, Quaranta V: Expression of matrix metalloprotease-2-cleaved laminin-5 in breast remodeling stimulated by sex steroids. Am J Pathol 1999, 154:1193–1201
20. Giannelli G, Falk-Marzillier J, Schiraldi O, Stetler-Stevenson WG, Quaranta V: Induction of cell migration by matrix metalloprotease-2 cleavage of laminin-5. Science 1997, 277:225–228
21. Schedin P, Mitrenga T, Kaeck M: Estrous cycle regulation of mammary epithelial cell proliferation, differentiation, and death in the Sprague-Dawley rat: a model for investigating the role of estrous cycling in mammary carcinogenesis. J Mammary Gland Biol Neoplasia 2000, 5:211–225
22. Lopez-De Leon A, Rojkind M: A simple micromethod for collagen and total protein determination in formalin-fixed paraffin-embedded sections. J Histochem Cytochem 1985, 33:737–743
23. Paine TM, Soule HD, Pauley RJ, Dawson PJ: Characterization of epithelial phenotypes in mortal and immortal human breast cells. Int J Cancer 1992, 50:463–473
24. Mehta RR, Graves JM, Hart GD, Shilkaitis A, Das Gupta TK: Growth and metastasis of human breast carcinomas with Matrigel in athymic mice. Breast Cancer Res Treat 1993, 25:65–71
25. Hettinger AM, Allen MR, Zhang BR, Goad DW, Malayer JR, Geisert RD: Presence of the acute phase protein, bikunin, in the endometrium

of gilts during estrous cycle and early pregnancy. Biol Reprod 2001, 65:507–513
26. Varella-Garcia M, Akduman B, Sunpaweravong P, Di Maria MV, Crawford ED: The UroVysion fluorescence in situ hybridization assay is an effective tool for monitoring recurrence of bladder cancer. Urol Oncol 2004, 22:16–19
27. Masso-Welch PA, Darcy KM, Stangle-Castor NC, Ip MM: A developmental atlas of rat mammary gland histology. J Mammary Gland Biol Neoplasia 2000, 5:165–185
28. Lund LR, Romer J, Thomasset N, Solberg H, Pyke C, Bissell MJ, Dano K, Werb Z: Two distinct phases of apoptosis in mammary gland involution: proteinase-independent and -dependent pathways. Development 1996, 122:181–193
29. Schedin PJ, Thackray LB, Malone P, Fontaine SC, Friis RR, Strange R: Programmed cell death and mammary neoplasia. Cancer Treat Res 1996, 83:3–22
30. Schedin PJ, Eckel-Mahan KL, McDaniel SM, Prescott JD, Brodsky KS, Tentler JJ, Gutierrez-Hartmann A: ESX induces transformation and functional epithelial to mesenchymal transition in MCF-12A mammary epithelial cells. Oncogene 2004, 23:1766–1779
31. Strange R, Li F, Saurer S, Burkhardt A, Friis RR: Apoptotic cell death and tissue remodelling during mouse mammary gland involution. Development 1992, 115:49–58
32. Wyllie AH, Kerr JF, Currie AR: Cell death: the significance of apoptosis. Int Rev Cytol 1980, 68:251–306
33. Stein T, Morris JS, Davies CR, Weber-Hall SJ, Duffy MA, Heath VJ, Bell AK, Ferrier RK, Sandilands GP, Gusterson BA: Involution of the mouse mammary gland is associated with an immune cascade and an acute-phase response, involving LBP, CD14 and STAT3. Breast Cancer Res 2004, 6:R75–R91
34. Monks J, Geske FJ, Lehman L, Fadok VA: Do inflammatory cells participate in mammary gland involution? J Mammary Gland Biol Neoplasia 2002, 7:163–176
35. Damsky C, Tremble P, Werb Z: Signal transduction via the fibronectin receptor: do integrins regulate matrix remodeling? Matrix Suppl 1992, 1:184–191
36. Thomasset N, Lochter A, Sympson CJ, Lund LR, Williams DR, Behrendtsen O, Werb Z, Bissell MJ: Expression of autoactivated stromelysin-1 in mammary glands of transgenic mice leads to a reactive stroma during early development. Am J Pathol 1998, 153:457–467
37. Werb Z, Ashkenas J, MacAuley A, Wiesen JF: Extracellular matrix remodeling as a regulator of stromal-epithelial interactions during mammary gland development, involution and carcinogenesis. Braz J Med Biol Res 1996, 29:1087–1097
38. Fridman R, Giaccone G, Kanemoto T, Martin GR, Gazdar AF, Mulshine JL: Reconstituted basement membrane (Matrigel) and laminin can enhance the tumorigenicity and the drug resistance of small cell lung cancer cell lines. Proc Natl Acad Sci USA 1990, 87:6698–6702
39. Fridman R, Kibbey MC, Royce LS, Zain M, Sweeney M, Jicha DL, Yannelli JR, Martin GR, Kleinman HK: Enhanced tumor growth of both primary and established human and murine tumor cells in athymic mice after coinjection with Matrigel. J Natl Cancer Inst 1991, 83:769–774
40. Fridman R, Sweeney TM, Zain M, Martin GR, Kleinman HK: Malignant transformation of NIH-3T3 cells after subcutaneous co-injection with a reconstituted basement membrane (Matrigel). Int J Cancer 1992, 51:740–744
41. Dumortier J, Daemi N, Pourreyron C, Anderson W, Bellaton C, Jacquier MF, Bertrand S, Chayvialle JA, Remy L: Loss of epithelial differentiation markers and acquisition of vimentin expression after xenograft with laminin-1 enhance migratory and invasive abilities of human colon cancer cells LoVo C5. Differentiation 1998, 63:141–150
42. Bix G, Iozzo RV: Matrix revolutions: "tails" of basement-membrane components with angiostatic functions. Trends Cell Biol 2005, 15:52–60
43. O'Reilly MS, Wiederschain D, Stetler-Stevenson WG, Folkman J, Moses MA: Regulation of angiostatin production by matrix metalloproteinase-2 in a model of concomitant resistance. J Biol Chem 1999, 274:29568–29571
44. Alexander CM, Selvarajan S, Mudgett J, Werb Z: Stromelysin-1 regulates adipogenesis during mammary gland involution. J Cell Biol 2001, 152:693–703
45. Nagy JA, Dvorak AM, Dvorak HF: VEGF-A(164/165) and PlGF: roles in angiogenesis and arteriogenesis. Trends Cardiovasc Med 2003, 13:169–175
46. Pettersson A, Nagy JA, Brown LF, Sundberg C, Morgan E, Jungles S, Carter R, Krieger JE, Manseau EJ, Harvey VS, Eckelhoefer IA, Feng D, Dvorak AM, Mulligan RC, Dvorak HF: Heterogeneity of the angiogenic response induced in different normal adult tissues by vascular permeability factor/vascular endothelial growth factor. Lab Invest 2000, 80:99–115
47. Mueller MM, Fusenig NE: Tumor-stroma interactions directing phenotype and progression of epithelial skin tumor cells. Differentiation 2002, 70:486–497
48. Shao ZM, Nguyen M, Barsky SH: Human breast carcinoma desmoplasia is PDGF initiated. Oncogene 2000, 19:4337–4345
49. Rosner B, Colditz GA, Willett WC: Reproductive risk factors in a prospective study of breast cancer: the Nurses' Health Study. Am J Epidemiol 1994, 139:819–835
50. Bonnier P, Romain S, Dilhuydy JM, Bonichon F, Julien JP, Charpin C, Lejeune C, Martin PM, Piana L: Influence of pregnancy on the outcome of breast cancer: a case-control study. Societe Francaise de Senologie et de Pathologie Mammaire Study Group. Int J Cancer 1997, 72:720–727
51. Albrektsen G, Heuch I, Hansen S, Kvale G: Breast cancer risk by age at birth, time since birth and time intervals between births: exploring interaction effects. Br J Cancer 2005, 92:167–175
52. Bladstrom A, Anderson H, Olsson H: Worse survival in breast cancer among women with recent childbirth: results from a Swedish population-based register study. Clin Breast Cancer 2003, 4:280–285
53. Whiteman MK, Hillis SD, Curtis KM, McDonald JA, Wingo PA, Marchbanks PA: Reproductive history and mortality after breast cancer diagnosis. Obstet Gynecol 2004, 104:146–154
54. Henderson BE, Ross R, Bernstein L: Estrogens as a cause of human cancer: the Richard and Hinda Rosenthal Foundation award lecture. Cancer Res 1988, 48:246–253
55. Rossouw JE, Anderson GL, Prentice RL, LaCroix AZ, Kooperberg C, Stefanick ML, Jackson RD, Beresford SA, Howard BV, Johnson KC, Kotchen JM, Ockene J: Risks and benefits of estrogen plus progestin in healthy postmenopausal women: principal results From the Women's Health Initiative randomized controlled trial. JAMA 2002, 288:321–333
56. Kroman N, Mouridsen HT: Prognostic influence of pregnancy before, around, and after diagnosis of breast cancer. Breast 2003, 12:516–521
57. Daling JR, Malone KE, Doody DR, Anderson BO, Porter PL: The relation of reproductive factors to mortality from breast cancer. Cancer Epidemiol Biomarkers Prev 2002, 11:235–241
58. Kang Y, Siegel PM, Shu W, Drobnjak M, Kakonen SM, Cordon-Cardo C, Guise TA, Massague J: A multigenic program mediating breast cancer metastasis to bone. Cancer Cell 2003, 3:537–549
59. van de Vijver MJ, He YD, van't Veer LJ, Dai H, Hart AA, Voskuil DW, Schreiber GJ, Peterse JL, Roberts C, Marton MJ, Parrish M, Atsma D, Witteveen A, Glas A, Delahaye L, van der Velde T, Bartelink H, Rodenhuis S, Rutgers ET, Friend SH, Bernards R: A gene-expression signature as a predictor of survival in breast cancer. N Engl J Med 2002, 347:1999–2009
60. Hadsell DL, Alexeenko T, Klemintidis Y, Torres D, Lee AV: Inability of overexpressed des(1-3)human insulin-like growth factor I (IGF-I) to inhibit forced mammary gland involution is associated with decreased expression of IGF signaling molecules. Endocrinology 2001, 142:1479–1488